

Low-frequency measurement of the tunneling amplitude in a flux qubit

M. Grajcar,^{1,*} A. Izmailkov,^{1,2} E. Il'ichev,^{1,†} Th. Wagner,¹ N. Oukhanski,¹ U. Hübner,¹
T. May,¹ I. Zhilyaev,^{1,‡} H.E. Hoenig,¹ Ya.S. Greenberg,^{3,§} V.I. Shnyrkov,^{3,¶}
D. Born,¹ W. Krech,³ H.-G. Meyer,¹ Alec Maassen van den Brink,⁴ and M.H.S. Amin⁴

¹*Institute for Physical High Technology, P.O. Box 100239, D-07702 Jena, Germany*

²*Moscow Engineering Physics Institute (State University), Kashirskoe sh. 31, 115409 Moscow, Russia*

³*Friedrich Schiller University, Institute of Solid State Physics, D-07743 Jena, Germany*

⁴*D-Wave Systems Inc., 320-1985 West Broadway, Vancouver, B.C., V6J 4Y3 Canada*

(Dated: January 9, 2022)

We have observed signatures of resonant tunneling in an Al three-junction qubit, inductively coupled to a Nb LC tank circuit. The resonant properties of the tank oscillator are sensitive to the effective susceptibility (or inductance) of the qubit, which changes drastically as its flux states pass through degeneracy. The tunneling amplitude is estimated from the data. We find good agreement with the theoretical predictions in the regime of their validity.

PACS numbers: 85.25.Cp, 85.25.Dq, 84.37.+q, 03.67.Lx

Several groups, using different devices, have by now established that superconductors can behave as macroscopic quantum objects.^{1–3} These are natural candidates for a qubit, the building block of a quantum computer.

Qubits are effectively two-level systems with time-dependent parameters. One of them is a superconducting loop with low inductance L , including three Josephson junctions (a 3JJ qubit).⁴ Its potential energy, $U = \sum_{j=1}^3 E_{Jj}(\phi_j)$, depends on the Josephson phase differences ϕ_j across the junctions. Due to flux quantization $\sum_{j=1}^3 \phi_j = 2\pi\Phi_x/\Phi_0$ (with Φ_x the external magnetic flux and $\Phi_0 = h/2e$ the flux quantum), only two ϕ_j 's are independent.

For suitable parameters, $U(\phi_1, \phi_2)$ has two minima corresponding to qubit states Ψ^l and Ψ^r , carrying opposite supercurrents around the loop. These become degenerate for $\Phi_x = \frac{1}{2}\Phi_0$. The Coulomb energy E_C ($\equiv e^2/2C$, with C the capacitance of junction 1) introduces quantum uncertainty in the ϕ_j . Hence, near degeneracy the system can tunnel between the two potential minima. (Since $E_C \ll E_J \equiv E_{J1}$, we deal with a *flux* qubit; $E_C \gg E_J$ yields a *charge* qubit. Coherent tunneling was demonstrated in both.)

In the basis $\{\Psi^l, \Psi^r\}$ and near $\Phi_x = \frac{1}{2}\Phi_0$, the qubit can be described by the Hamiltonian

$$H(t) = -\epsilon(t)\sigma_z - \Delta\sigma_x; \quad (1)$$

Δ is the tunneling amplitude. At bias $\epsilon = 0$ the two lowest energy levels of the qubit anticross [Fig. 1(a)], with a gap of 2Δ . Increasing ϵ slowly enough, the qubit can adiabatically transform from Ψ^l to Ψ^r , staying in the ground state E_- . Since $dE_-/d\Phi_x$ is the persistent loop current, the curvature $d^2E_-/d\Phi_x^2$ is related to the qubit's susceptibility. Hence, near degeneracy the latter will have a peak, with a width given by $|\epsilon| \lesssim \Delta$.⁵ We present data demonstrating such behavior in an Al 3JJ qubit.

Our technique is similar to rf-SQUID readout.^{6,7} The qubit loop is inductively coupled to a parallel resonant tank circuit [Fig. 1(b)]. The tank is fed a monochro-

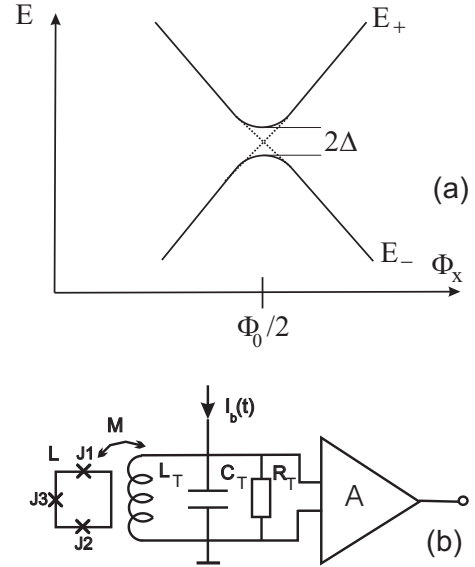


FIG. 1: (a) Quantum energy levels of the qubit vs external flux. The dashed lines represent the classical potential minima. (b) Phase qubit coupled to a tank circuit.

matic rf signal at its resonant frequency ω_T . Then both amplitude v and phase shift χ (with respect to the bias current I_b) of the tank voltage will strongly depend on (A) the shift in resonant frequency due to the change of the effective qubit inductance by the tank flux, and (B) losses caused by field-induced transitions between the two qubit states. Thus, the tank both applies the probing field to the qubit, and detects its response.

The output signal depends on the tank's quality factor Q . Using superconducting coil, values as high as $Q \sim 10^3$ can be obtained, leading to high readout sensitivity, e.g., in rf-SQUID magnetometers.⁸ Such a tank can therefore be used to probe phase qubits.⁹ For small L , the results are summarized by⁵

$$v = I_0\omega_T L_T Q / \sqrt{1 + (2Q\xi)^2}, \quad (2)$$

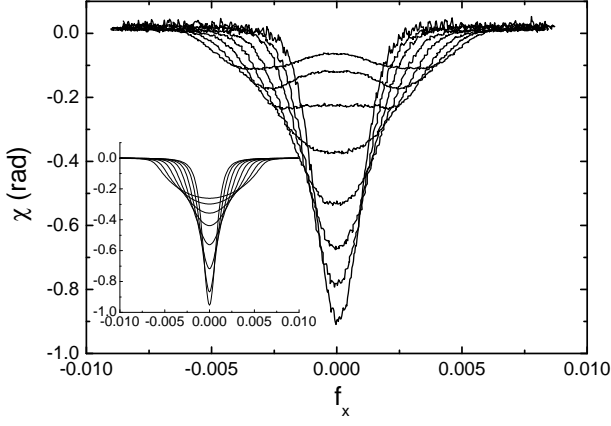


FIG. 2: Tank phase shift vs flux bias near degeneracy. From the lower to the upper curve (at $f_x = 0$) the driving-voltage amplitude $V_{dr} \equiv I_0 \omega_T L_T Q$ takes values 0.5, 1.0, 1.5, 1.9, 2.9, 3.5, 3.9 μV . Inset: theoretical curves for $\Delta/h = 650$ MHz, and $I_0 = 0.07, 0.13, 0.20, 0.26, 0.39, 0.47, 0.53$ nA.

$$\tan \chi = 2Q\xi, \quad (3)$$

$$\xi(v, f_x) = \frac{k^2 L}{2\Phi_0^2} \int_0^{2\pi} \frac{d\phi}{\pi} \cos^2 \phi \frac{d^2 E_-(f)}{df^2}, \quad (4)$$

$$f = f_x + \frac{Mv}{\omega_T L_T \Phi_0} \sin \phi, \quad (5)$$

where $f_x = \Phi_x/\Phi_0 - \frac{1}{2}$, I_0 is the bias-current amplitude, and $k = M/\sqrt{LL_T}$ is the tank-qubit coupling coefficient, with M (L_T) the mutual (tank) inductance. The ground-state curvature is¹⁰

$$\frac{d^2 E_-}{df^2} = -\frac{E_J^2 \Delta^2 \lambda^2}{(E_J^2 \lambda^2 f^2 + \Delta^2)^{3/2}}, \quad (6)$$

where $\lambda(\alpha, g)$ (with $g = E_J/E_C$) is the conversion factor in $\epsilon = E_J \lambda f$.¹¹ If I_0 vanishes, $\xi = \frac{1}{2} k^2 L d^2 E_- / d\Phi_x^2$ becomes an external parameter accounting for the qubit susceptibility coupled to the tank. For finite I_0 , this has to be averaged over a bias cycle $0 < \phi < 2\pi$. The resulting integral (4) turns out to involve a weight $\cos^2 \phi$, since the effective time-dependent coupling is $(k\dot{f})^2$ [cf. the ϕ -derivative of Eq. (5)], proportional to the square of the voltage the tank induces in the qubit. The resulting equations are coupled and nonlinear, but readily solved numerically.

For the tank, we prepared a square-shape Nb pancake coil on an oxidized Si substrate. The line width of the 20 windings was 2 μm , with a 2 μm spacing. Predefined alignment marks allow placing a qubit in the center. For flexibility, only the coil was made lithographically; an external capacitance C_T is used to change ω_T in the range 5–35 MHz. For the selected tank ($L_T \approx 50$ nH, $C_T \approx 470$ pF), we obtained $\omega_T/2\pi = 32.675$ MHz and $Q \approx 725$ from the voltage-frequency characteristic.

The 3JJ qubit structure was manufactured out of Al by conventional shadow evaporation. The area of two of the junctions was estimated using electron microscopy

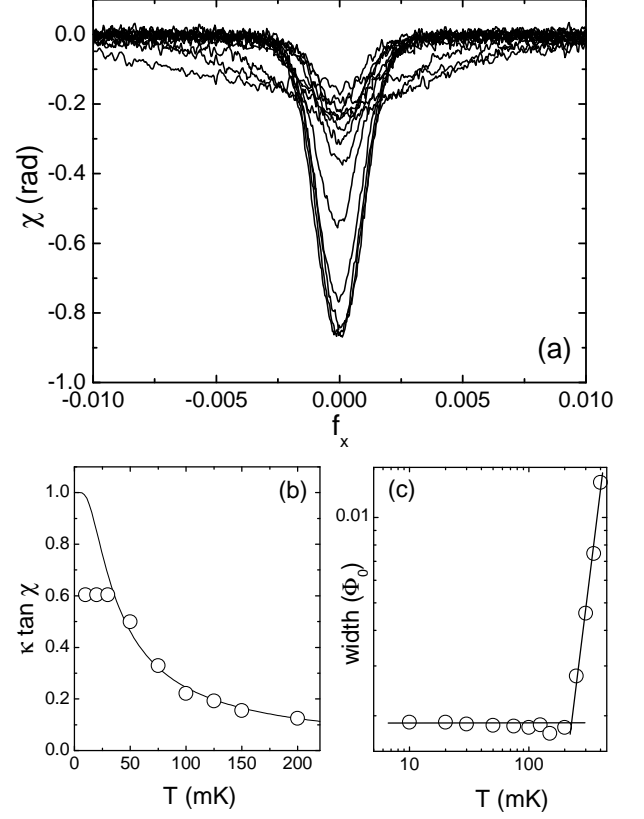


FIG. 3: (a) Tank phase shift vs flux bias near degeneracy and for $V_{dr} = 0.5$ μV . From the lower to the upper curve (at $f_x = 0$) the temperature is 10, 20, 30, 50, 75, 100, 125, 150, 200, 250, 300, 350, 400 mK. (b) Normalized amplitude of $\tan \chi$ (circles) and $\tanh(\Delta/k_B T)$ (line), for the Δ following from Fig. 2; the overall scale κ is a fitting parameter. The data indicate a saturation of the effective qubit temperature at 30 mK. (c) Full dip width at half the maximum amplitude vs temperature. The horizontal line fits the low- T (< 200 mK) part to a constant; the sloped line represents the T^3 behavior observed empirically for higher T .

as 190×650 nm² while one is smaller, so that $\alpha \equiv E_{J3}/E_{J1,2} \approx 0.8$. The critical current was determined by measuring an rf-SQUID prepared on the same chip⁷ as $I_c = 2eE_J/\hbar \approx 380$ nA. With $E_C/h \approx 3$ GHz, one finds $g \approx 60$ and $\lambda \approx -4.4$. The loop area was 90 μm^2 , with $L = 38$ pH. We measured v by a three-stage cryogenic amplifier, placed at ≈ 2 K and based on commercial pseudomorphic high electron mobility transistors. It was slightly modified from the version in Ref. 12 to decrease its back-action on the qubit. The input-voltage noise was < 0.6 nV/ $\sqrt{\text{Hz}}$ in the range 1–35 MHz. The noise temperature was ~ 300 mK at 32 MHz. The effective qubit temperature due to the amplifier's back-action should be considerably lower because of the small $k \approx 2 \cdot 10^{-2}$.

The $\chi(f_x)$ curves measured at various I_0 and a mixing-chamber temperature $T = 10$ mK are shown in Fig. 2. The narrow dip at $f_x = 0$ directly corresponds to the

one in Eq. (6), in line with the qualitative picture below Eq. (1). With device parameters as above, all quantities in Eqs. (2)–(6) are known, but Δ only in principle: its exponential sensitivity to α and especially g makes it notoriously hard to calculate *a priori*. Hence, it is treated as a free parameter; calculated curves for the best fit $\Delta/h = 650$ MHz are shown in the inset. For the largest I_0 the experimental and theoretical curves disagree, for the rapid change of Φ_x then leads to Landau–Zener transitions^{13,14} suppressing the dip.

The T -dependence of χ is shown in Fig. 3. For increasing T the dip’s amplitude decreases while, strikingly, its width is unchanged [Fig. 3(c)]. Both are a simple manifestation of the Hamiltonian (1) yielding $\langle\sigma_z\rangle = (\epsilon/\Omega) \times \tanh(\Omega/k_B T)$,¹⁵ $\Omega = \sqrt{\epsilon^2 + \Delta^2}$. This result of equilibrium statistics of course assumes that the t -dependence of $\epsilon(t)$ is adiabatic. However, it *does* remain valid if the full (Liouville) evolution operator of the qubit would contain standard Bloch-type relaxation and dephasing terms (which indeed are not probed⁵) in addition to the Hamiltonian dynamics (1), since the fluctuation–dissipation theorem guarantees that such terms do not affect equilibrium properties. Normalized dip amplitudes are shown vs T in Fig. 3(b) together with $\tanh(\Delta/k_B T)$,

for $\Delta/h = 650$ MHz *independently* obtained above from the low- T width. The good agreement strongly supports our interpretation, and is consistent with Δ being T -independent in the relevant range.¹⁶ Of course, for higher T the dip will wash out; we observe a width $\propto T^3$ above a crossover temperature ≈ 225 mK. For T of this order, deviations from the two-state model can be expected, especially for $f_x \neq 0$. This behavior outside the qubit regime has not been pursued.

In conclusion, we have observed resonant tunneling in a macroscopic superconducting system, containing an Al flux qubit and a Nb tank circuit. The latter played dual control and readout roles. The impedance readout technique allows direct characterization of some of the qubit’s quantum properties, *without* using spectroscopy.^{2,3} In a range 50–200 mK, the *effective* qubit temperature has been verified [Fig. 3(b)] to be the same as the mixing chamber’s (after Δ has been determined at low T), which is often difficult to confirm independently.

MHSA and AMvdB are grateful to A.Yu. Smirnov and A.M. Zagoskin for fruitful discussions, and to P.C.E. Stamp for the remark on effective thermometry. MG wants to acknowledge partial support by the Slovak Grant Agency VEGA (Grant No. 1/9177/02).

* On leave from Department of Solid State Physics, Comenius University, SK-84248 Bratislava, Slovakia.

† Electronic address: ilichev@ipht-jena.de

‡ On leave from Inst. of Microelectronic Technology, Russian Academy of Science, 142432 Chernogolovka, Russia.

§ On leave from Novosibirsk State Technical University, 20 K. Marx Ave., 630092 Novosibirsk, Russia.

¶ On leave from B. Verkin Inst. for Low Temperature Physics and Engineering, 310164 Kharkov, Ukraine.

¹ Y. Nakamura, Yu.A. Pashkin, and J.S. Tsai, *Nature* **398**, 786 (1999); J.R. Friedman, V. Patel, W. Chen, S.K. Tolpygo, and J.E. Lukens, *Nature* **406**, 43 (2000); D. Vion, A. Aassime, A. Cottet, P. Joyez, H. Pothier, C. Urbina, D. Esteve, and M.H. Devoret, *Science* **296**, 886 (2002); J.M. Martinis, S. Nam, J. Aumentado, and C. Urbina, *Phys. Rev. Lett.* **89**, 117901 (2002).

² C.H. van der Wal, A.C.J. ter Haar, F.K. Wilhelm, R.N. Schouten, C.J.P.M. Harmans, T.P. Orlando, S. Lloyd, and J.E. Mooij, *Science* **290**, 773 (2000).

³ E. Il’ichev, N. Oukhanski, A. Izmalkov, Th. Wagner, M. Grajcar, H.-G. Meyer, A.Yu. Smirnov, A. Maassen van den Brink, M.H.S. Amin, and A.M. Zagoskin, *Phys. Rev. Lett.* **91**, 097906 (2003).

⁴ J.E. Mooij, T.P. Orlando, L. Levitov, L. Tian, C.H. van der Wal, and S. Lloyd, *Science* **285**, 1036 (1999).

⁵ Ya.S. Greenberg, A. Izmalkov, M. Grajcar, E. Il’ichev, W. Krech, H.-G. Meyer, M.H.S. Amin, and A. Maassen van den Brink, *Phys. Rev. B* **66**, 214525 (2002).

⁶ A.H. Silver and J.E. Zimmerman, *Phys. Rev.* **157**, 317 (1967).

⁷ E. Il’ichev *et al.*, *Rev. Sci. Instrum.* **72**, 1882 (2001).

⁸ V.V. Danilov and K.K. Likharev, *Zh. Tekh. Fiz.* **45**, 1110 (1975) [*Sov. Phys. Tech. Phys.* **20**, 697 (1976)].

⁹ Ya.S. Greenberg, A. Izmalkov, M. Grajcar, E. Il’ichev,

W. Krech, and H.-G. Meyer, *Phys. Rev. B* **66**, 224511 (2002).

¹⁰ A minus sign is missing in Eq. (17) of Ref. 5.

¹¹ Let us rectify the discussion of λ , Eq. (12) in Ref. 5. In Eq. (1) of Ref. 2, ϵ is expressed in terms of the persistent current (subsequently given numerically for their sample parameters) instead of E_J , which implicitly incorporates λ . In T.P. Orlando *et al.*, *Phys. Rev. B* **60**, 15398 (1999), the flux–energy conversion is carried out in Eq. (32) and Appendix B. Our λ differs from their r_1/E_J only in an $\mathcal{O}(g^{-1/2})$ correction [taken into account below our Eq. (6)], plus an overall sign immaterial for λ^2 . This correction *decreasing* λ (here by $\sim 9\%$) may be small, but it has a clear interpretation: as f_x increases, the upper well, ultimately losing classical stability, becomes softer. Hence, its local zero-point energy decreases, slightly counteracting the rise of the potential minimum.

¹² N. Oukhanski, M. Grajcar, E. Il’ichev, and H.-G. Meyer, *Rev. Sci. Instrum.* **74**, 1145 (2003).

¹³ L.D. Landau, *Z. Phys. Sowjetunion* **2**, 46 (1932); C. Zener, *Proc. R. Soc. London A* **137**, 696 (1932).

¹⁴ A. Izmalkov *et al.*, cond-mat/0307506, to appear in *Europhys. Lett.*

¹⁵ Using this simple tanh law also for the net qubit response $\propto \partial_\epsilon \langle\sigma_z\rangle$ accounts for the following subtlety. While our method is quasi-equilibrium, *on the scale of one bias cycle* $\sim \omega_T^{-1}$ relaxation is slow. Hence, in the finite- T generalization, flux derivatives such as in Eq. (6) become adiabatic rather than isothermal. For finite T and v , the problem is essentially nonequilibrium and outside our scope.

¹⁶ S.-X. Li, Y. Yu, Y. Zhang, W. Qiu, S. Han, and Z. Wang, *Phys. Rev. Lett.* **89**, 098301 (2002) and references therein.